Biochemistry and Biophysics Reports 21 (2020) 100738

Contents lists available at ScienceDirect

Biochemistry and Biophysics Reports

journal homepage: www.elsevier.com/locate/bbrep

Regenerating islet-derived protein (Reg)3β plays a crucial role in attenuation of ileitis and colitis in mice

Ryodai Shindo[a,1], Takaharu Katagiri[a,b,1], Sachiko Komazawa-Sakon[a], Masaki Ohmuraya[c], Wakami Takeda[d], Yoshiko Nakagawa[e], Naomi Nakagata[e], Tetsushi Sakuma[f], Takashi Yamamoto[f], Chiharu Nishiyama[d], Takashi Nishina[a], Soh Yamazaki[a], Hideto Kameda[b], Hiroyasu Nakano[a,g,*]

[a] Department of Biochemistry, Toho University Graduate School Medicine, 5-21-16 Omori-Nishi, Ota-ku, Tokyo, 143-8540, Japan
[b] Division of Rheumatology, Department of Internal Medicine, Ohashi Medical Center, 2-22-36 Ohashi, Meguro-ku, Tokyo, 153-8515, Japan
[c] Department of Genetics, Hyogo College of Medicine, Nishinomiya, Hyogo, 663-8501, Japan
[d] Laboratory of Molecular Biology and Immunology, Department of Biological Science and Technology, Faculty of Industrial Science and Technology, Tokyo University of Science, 6-3-1 Niijuku, Katsushika-ku, Tokyo, 125–8585, Japan
[e] Center for Animal Resources and Development, Kumamoto University, 2–2–1 Honjo, Chuo-ku, Kumamoto, 860-0811, Japan
[f] Division of Integrated Sciences for Life, Graduate School of Integrated Sciences for Life, Hiroshima University, 1-3-1 Kagamiyama, Higashi-Hiroshima, Hiroshima, 739-8526, Japan
[g] Host Defense Research Center, Toho University School of Medicine, 5-21-16 Omori-Nishi, Ota-ku, Tokyo, 143-8540, Japan

ARTICLE INFO

Keywords:
Cellular FLICE-Inhibitory protein
Colitis
Dextran sulfate sodium
Ileitis
Regenerating islet-derived protein

ABSTRACT

Regenerating islet-derived protein (Reg)3β belongs to a member of the Reg family of proteins and has pleiotropic functions, including antimicrobial activity and tissue repair. However, whether Reg3β plays a protective role in the development of colitis and ileitis has not been fully investigated. We generated transgenic mice expressing a short form of cellular FLICE-inhibitory protein (cFLIPs) that promotes necroptosis, a regulated form of cell death. cFLIPs transgenic (*CFLARs* Tg) mice develop severe ileitis in utero. Although Reg3β is undetectable in the small intestine of wild-type embryos, its expression is aberrantly elevated in the small intestine of *CFLARs* Tg embryos. To test whether elevated Reg3β attenuates or exacerbates ileitis in *CFLARs* Tg mice, we generated a *Reg3b*$^{-/-}$ strain. *Reg3b*$^{-/-}$ mice grew to adulthood without apparent abnormalities. Deletion of *Reg3b* in *CFLARs* Tg mice exacerbated the embryonic lethality of *CFLARs* Tg mice. Dextran sulfate sodium-induced colitis, characterized by body weight loss and infiltration of neutrophils, was exacerbated in *Reg3b*$^{-/-}$ compared to wild-type mice. Moreover, the expression of *Interleukin 6*, an inflammatory cytokine and *Chitinase-like 3*, a marker for tissue repair macrophages was elevated in the colon of *Reg3b*$^{-/-}$ mice compared to wild-type mice after DSS treatment. Together, these results suggest that attenuation of colitis and ileitis is a result of Reg3β's real function.

1. Introduction

Regenerating islet-derived proteins (Regs) comprise the superfamily of C-type lectin proteins encoded by *Reg1*, *Reg2*, *Reg3a*, *Reg3b*, *Reg3g*, *Reg3d*, and *Reg4* [1,2]. The Reg family proteins are expressed in various tissues and have pleiotropic functions. *Reg3b* and *Reg3g* encode murine Reg3β and Reg3γ, respectively, and are murine homolog of human REG3A. Both proteins are highly expressed in the small intestine of adult mice at both mRNA and protein levels, but their expression is very low in the colon. Intriguingly, expression of Reg3β and Reg3γ is not detectable in the embryonic mouse intestine but gradually increases along with colonization of the commensal bacteria after birth [3].

Reg3β promotes tissue repair of ischemic heart injury through recruiting macrophages and pancreatic tumor growth by skewing M2-

Abbreviations: Arg1, Arginase-1; *CFLARs* Tg, cFLIPs transgenic; cFLIPs and $_L$, cellular FLICE-inhibitory protein, short and long forms; Chitinase-like 3, Chil3; DSS, dextran sulfate sodium; GFP, green fluorescent protein; IECs, intestinal epithelial cells; IL, interleukin; ILC3, group 3 innate lymphoid cell; Mrc1, Mannose receptor C-type 1; MLKL, mixed lineage kinase domain–like protein; pSTAT3, phospho-STAT3; qPCR, quantitative polymerase chain reaction; Reg, regenerating islet-derived protein; RIPK, receptor-interacting protein kinase; Retnla, Resistin-like alpha; RORγt, RAR-related orphan receptor gamma t; STAT, signal transducer and activator of transcription

* Corresponding author. Department of Biochemistry, Toho University Graduate School Medicine, 5-21-16 Omori-Nishi, Ota-ku, Tokyo, 143-8540, Japan.
E-mail address: hiroyasu.nakano@med.toho-u.ac.jp (H. Nakano).

[1] These authors contributed equally to this work.

https://doi.org/10.1016/j.bbrep.2020.100738
Received 19 November 2019; Received in revised form 26 December 2019; Accepted 25 January 2020

type macrophages [4,5]. M2-type macrophages express several markers, including Arginase 1 (Arg1), Mannose receptor C-type 1 (Mrc1), Resistin-like alpha (Retnla), and Ym1, and are critically involved in tissue repair process [6]. *Reg3g*$^{-/-}$ mice are highly susceptible to bacterial infection [7], suggesting that Reg3γ restricts the invasion of pathogenic bacteria under homeostatic conditions. *Reg3b* and *Reg3g* expression is upregulated by interleukin (IL)-6 and IL-22 in a signal transducer and activator of transcription (STAT)3-dependent manner [8]. T_H17 cells and group 3 innate lymphoid cells (ILC3s) are major sources of IL-22 in the intestine [9,10]. T_H17 cells and ILC3s express a transcription factor, RAR-related orphan receptor gamma t (RORγt), which is encoded by *Rorc* and essential for their development [9,10]. Accordingly, the expression of IL-22 is severely diminished in the intestine of *Rorc*$^{-/-}$ mice. We previously reported that expression of *Reg3b* and *Reg3g* is abolished in the small intestine of *Rorc*$^{-/-}$ and *Il22*$^{-/-}$ animals, but not in *Rag2*$^{-/-}$ mice [11]. Thus, ILC3-dependent IL-22 production is crucial for upregulation of *Reg3b* and *Reg3g*, but T_H17 cell-dependent production is not.

Apoptosis is a form of programmed or regulated cell death that is executed by activation of caspases [12]. Recent studies have focused on necroptosis, another form of regulated form of cell death [13,14] that is crucial in the development of ischemia-reperfusion injury and elimination of some viruses. Various agents, including tumor necrosis factor, FasL, TRAIL, polyinosinic-polycytidylic acid, and viral infection, induce necroptosis. Necroptosis is executed by sequential phosphorylation of receptor-interacting protein kinase (RIPK)1, RIPK3, and an executioner protein of necroptosis called mixed lineage kinase domain–like protein (MLKL). The phosphorylated form of MLKL undergoes oligomerization and then translocates to the plasma membrane, resulting in membrane pore formation. Activation of caspase 8 blocks the necroptotic pathway through cleavage and inactivation of RIPK1 and RIPK3 under physiological conditions [13,14]. Cellular FLICE-inhibitory protein (cFLIP) is a caspase 8–like protein but lacks cysteine protease activity, so that cFLIP binds to and suppresses caspase 8 activation [15,16]. cFLIP consists of a short form (cFLIPs) and long form ($cFLIP_L$) because of alternative splicing, and the forms are encoded by *CFLARs* and *CFLAR*$_L$, respectively. $cFLIP_L$ blocks both apoptosis and necroptosis, whereas cFLIPs blocks apoptosis but promotes necroptosis [17,18].

We recently reported that mice expressing *CFLARs* on the X chromosome develop severe ileitis and that male *CFLARs* Tg mice die before or around birth because of severe ileitis [11]. The expression of Reg3β and Reg3γ is aberrantly elevated in the embryonic small intestine of *CFLARs* Tg animals but not in wild-type mice [11]. Given that deletion of *Rorc* or *Il22* substantially rescues the lethal phenotype of *CFLARs* Tg mice [11], aberrantly activated ILC3s are primarily responsible for intestinal injury. However, it is unclear whether the elevated *Reg3b* or *Reg3g per se* attenuates or exacerbates ileitis in *CFLARs* Tg mice. To address this issue, we generated *Reg3b*$^{-/-}$ animals and found that deletion of *Reg3b* increased embryonic lethality in *CFLARs* Tg mice. Moreover, we found that dextran sulfate sodium (DSS)-induced colitis was exacerbated in *Reg3b*$^{-/-}$ mice. Together, these results suggest that attenuation of colitis and ileitis is a result of Reg3β's real function.

2. Materials and methods

2.1. Reagents

The following antibodies used in this study were obtained from the indicated sources: anti-green fluorescent protein (GFP) (Go-Af1480, Frontier Institute), anti-Reg3β (AF5110, R&D Systems), anti-Reg3γ (provided by H. Kiyama), anti-phospho-STAT3 (9131, Cell Signaling), anti-STAT3 (sc-482, Santa Cruz), anti-β-tubulin (T5168, Sigma-Aldrich), anti-CD45.2 (104, BioLegend), anti-CD11b (M1/70, TONBO Biosciences), and anti-Ly-6G (1A8, TONBO Biosciences). Horseradish peroxidase-conjugated donkey anti-rabbit IgG (NA934) and sheep anti-mouse IgG (NA931) antibodies were purchased from GE Healthcare Life Sciences. Alexa Fluor 594–conjugated donkey anti-rabbit immunoglobulin G (IgG) (A21207) and Alexa Fluor 488–conjugated donkey anti-goat IgG (A11055) antibodies were from Invitrogen.

2.2. Mice

C57/BL6J mice were purchased from CLEA-Japan. *Rorc-gfp* reporter (*Rorc-gfp/gfp*) mice [19] were provided by K. Honda under a third-party transfer agreement with the Jackson Laboratory. *CFLARs* Tg mice have been described previously [11]. All animal experiments were performed according to the guidelines approved by the Institutional Animal Experiments Committee of Toho University School of Medicine.

2.3. Generation of *Reg3b*$^{-/-}$ and *Reg3g*$^{-/-}$ mice by the CRISPR-Cas9 method

A detailed strategy for generating *Reg3b*$^{-/-}$ and *Reg3g*$^{-/-}$ mice by the *CRISPR-Cas9* method has been described previously [20]. Among several lines harboring a deletion of the *Reg3b* and *Reg3g* genes, we established two lines of *Reg3b*$^{-/-}$ mice and two lines of *Reg3g*$^{-/-}$ mice. *Reg3b*$^{-/-}$ and *Reg3g*$^{-/-}$ mice were backcrossed with C57/BL6J animals for at least four generations. To generate *CFLARs* Tg;*Reg3b*$^{-/-}$ mice, we crossed female *CFLARs* Tg mice with male *Reg3b*$^{-/-}$ mice. Primers for genotyping of these mice are described in Table S1.

2.4. Histological, immunohistochemical, and immunofluorescent analysis

To detect RORγt$^+$ cells by immunofluorescent analysis, we crossed *CFLARs* Tg mice with *Rorc-gfp/gfp* mice, in which GFP expression is under the control of the endogenous *Rorc* gene promoter [19]. The small intestine was removed from *Rorc-gfp/+*, male *CFLARs Tg;Rorc-gfp/+*, and female *CFLARs* Tg;*Rorc-gfp/+* animals at embryonic day 18.5 (E18.5) and fixed in 10% formalin phosphate-buffered saline (PBS). Paraffin-embedded sections were stained with anti-GFP (to detect RORγt$^+$ cells), anti-Reg3β, and anti-phospho-STAT3 (pSTAT3) antibodies and visualized by the respective Alexa Fluor–conjugated secondary antibodies. We used the tyramide signal amplification method to increase the signals of pSTAT3 according to the manufacturer's instructions (NEL741001KT, PerkinElmer). Pictures were obtained by a confocal microscopy (Nikon). Images were analyzed with NIS-Elements AR Analysis software (Nikon).

The small intestines and colons of 8- to 12-week-old wild-type, *Reg3b*$^{-/-}$, and *Reg3g*$^{-/-}$ mice were fixed in 10% formalin PBS. Paraffin-embedded sections were stained with hematoxylin and eosin (H&E) or immunostained with anti-Reg3β antibody, and visualized by HRP-conjugated donkey anti-rabbit IgG. Pictures were obtained using an All in One microscope (BZ-X710, KEYENCE), and images were analyzed with KEYENCE software (KEYENCE).

2.5. Quantitative polymerase chain reaction (qPCR)

Total RNA from the small intestine and colon was prepared from 8- to 12-week-old mice, and cDNA was synthesized with the Revertra Ace qPCR RT Kit (Toyobo). qPCR analysis of the target genes was performed with the 7500 Real-Time PCR detection system with the SYBR green method and an endogenous control, murine *Hprt*, with 7500 SDS software (Applied Biosystems). The amounts of each gene were calculated relative to those of murine *Hprt* with 7500 SDS software (Applied Biosystems). The following primers were used in this study: *Arg1*, 5′-CCACACACCTGTAAGCCAGG-3′ and 5′-CAGTACTTGATGGTCCTT CCG-3'; *Chil3*, 5′-AAAGACAAGAACACTGAGCTAAAAACTC-3′ and 5′-GAATCTGATAACTGACTGAATGAATATC-3'; *Hprt*, 5′- AACAAAGTCT GGCCTGTATCCAA -3′ and 5′-GCAGTACAGCCCCAAAATGG-3'; *Il6*, 5′-GTATGAACAACGATGATGCACTTG-3′ and 5′- ATGGTACTCCAGAA GACCAGAGGA-3'; *Il11*, 5′-CTGCACAGATGAGAGACAAATTCC-3′ and 5′-GAAGCTGCAAAGATCCCAATG-3'; *Il17a*, 5′-CTGGAGGATAACACTG

TGAGAGT-3′ and 5′- TGCTGAATGGCGACGGAGTTC-3'; *Il22*, 5′-TCCG AGGAGTCAGTGCTAAA-3′ and 5′-AGAACGTCTTCCAGGGTGAA-3'; *Mrc1*, 5′-TCTTGTTTGTCCCAGGCAAGG-3′ and 5′-ACCCAGTTATGCAA ATTTACAGG-3'; *Reg3b*, 5′-CTCCTGCCTGATGCTCTTAT-3′ and 5′-TTG TTACTCCATTCCCATCC-3'; and *Reg3g*, 5′-ACGAATCCTTCCTCTTCCT CAG-3′ and 5′-GTCTTCACATTTGGGATCTTG-C-3'; *Retnla*, 5′-ATCTTG GGAGATCCAGAGTGG-3′ and 5′-TCAAAGCTGGGTTCTCCACC-3'.

2.6. Western blotting

Murine tissues were homogenized with a Polytron (KINEMATICA) and lysed in RIPA buffer [50 mM Tris-HCl (pH 8.0), 150 mM NaCl, 1% Nonidet P-40, 0.5% deoxycholate, 0.1% SDS, 25 mM β-glycerophosphate, 1 mM sodium orthovanadate, 1 mM sodium fluoride, 1 mM phenylmethylsulfonyl fluoride, 1 μg/ml aprotinin, 1 μg/ml leupeptin, and 1 μg/ml pepstatin]. After centrifugation, cell lysates were subjected to SDS polyacrylamide gel electrophoresis and transferred onto polyvinylidene difluoride membranes (IPVH 00010, Millipore). The membranes were analyzed by immunoblotting with the indicated antibodies and developed with Super Signal West Dura Extended Duration Substrate (34076, Thermo Scientific). The signals were analyzed using an Amersham Imager 600 (GE Healthcare Life Sciences).

2.7. Induction of DSS-induced colitis

Eight-to twelve-week-old male wild-type (C57BL/6J) and *Reg3b*$^{-/-}$ mice (9–10 mice per group) were administered with 1.5% DSS (MW: 36,000–50,000 D; MP Biomedicals) *ad libitum* in drinking water for 5 days, which then was changed to regular drinking water. Control wild-type C57/BL6 mice were cohoused with *Reg3b*$^{-/-}$ mice for at least 2 weeks to adjust the composition of the commensal microbiota before DSS administration. When animals lost 20% of initial body weight or were unable to take food or water on their own, they were immediately euthanized by cervical dislocation. The colons of mice that did not lose 20% body weight were removed on day 8 or 13 after DSS treatment and subjected to flow cytometric analysis and histological analysis, respectively.

2.8. Preparation of lamina propria cells from the colon

Lamina propria cells were prepared from colon samples of DSS-treated mice on day 8 as described previously [21]. Briefly, after removal of mucosa and epithelial cells by incubating in the presence of EDTA (1 mM), the intestine was cut into small fragments and digested with collagenase (1 mg/ml, Wako). Cells were filtered using nylon mesh, suspended in a 40% Percoll solution (GE Healthcare), and placed in an 80% Percoll solution. After centrifugation for 20 min at 880 × *g* at room temperature, cells at the interface of 40% and 80% Percoll were harvested and analyzed by flow cytometry.

2.9. Flow cytometry analysis

Cells were stained with anti-CD45.2, anti-CD11b, and anti-Ly-6G in flow cytometry staining buffer (eBioscience). Fixable Viability Dye eFluor 506 (65-0816-14, eBioscience) was used to distinguish live from dead cells, and live cells were analyzed using LSR Fortessa X-20 cell analyzer (BD Bioscience) and FlowJo (BD Biosciences).

2.10. Statistical analysis

Statistical significance was determined using the two-tailed unpaired Student *t*-test or repeated measures ANOVA. *$P < 0.05$ was considered to be statistically significant.

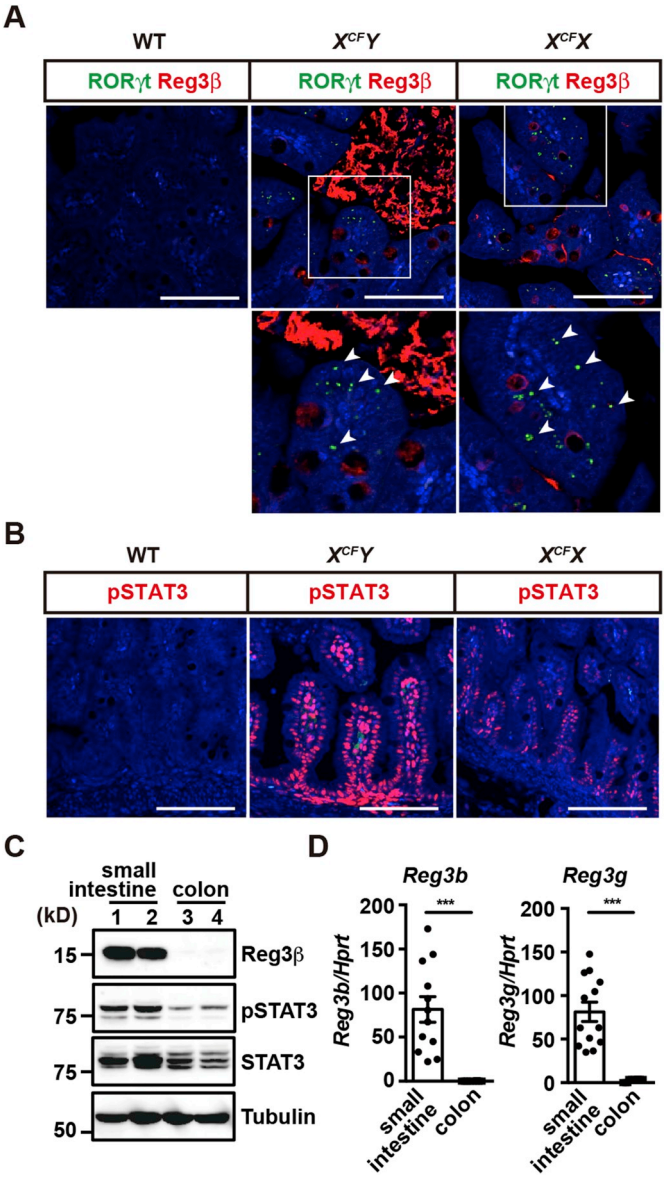

Fig. 1. Expression of Reg3β and infiltration of RORγt$^+$ cells in the small intestine of *CFLARs* Tg mice at the embryonic stage. (A, B) Small intestine sections from wild-type (WT), *X*^{CF}*Y*, and *X*^{CF}*X* mice on a *Rorc-gfp/+* genetic background at E18.5 were stained with anti-GFP (green) and anti-Reg3β (red) (A), or anti-pSTAT3 antibodies (magenta) (B). Lower panels are enlarged images of white boxes in the upper panels (A). White arrowheads indicate RORγt$^+$ cells. Scale bars, 100 μm. (C) Expression of Reg3β in the small intestine and colon of adult wild-type mice. Tissue extracts were prepared from the small intestine and colon of 8- to 12-week-old wild-type mice and examined by Western blotting with the indicated antibodies. Each number indicates an individual mouse. Results represent two independent experiments. (D) mRNA was prepared from the small intestine and colon of 8- to 12-week-old mice, and the expression of *Reg3b* and *Reg3g* was determined by qPCR. Results are mean ± SEM (n = 12 mice). Statistical significance was determined using the two-tailed unpaired Student's *t*-test. ***$P < 0.001$.

3. Results

3.1. Characterization of the expression of Reg3β in the intestine of embryos and adult mice

Because GFP is expressed under the control of the endogenous promoter of *Rorc* in *Rorc-gfp* reporter mice [19], RORγt$^+$ cells (ILC3s and T_H17 cells) are recognized as GFP$^+$ cells. We previously reported

that the expression of Reg3β is elevated in the small intestine of embryos of *CFLARs* Tg mice, but not in wild-type animals [11]. To investigate further the relationship between infiltration of RORγt$^+$ cells and the expression of Reg3β, we analyzed the small intestine of wild-type and *CFLARs* Tg mice at E18.5 by immunofluorescent analysis. Male and female *CFLARs* Tg mice are referred to as $X^{CF}Y$ and $X^{CF}X$ mice, respectively, hereafter.

We found that RORγt$^+$ cells accumulated and that intestinal epithelial cells (IECs) expressed Reg3β in the small intestine of *CFLARs* Tg embryos, but not in wild-type mice (Fig. 1A). Reg3β-positive signals were also detected in the lumen of the small intestine, suggesting that Reg3β protein was secreted from IECs and accumulated there (Fig. 1A). Moreover, we detected pSTAT3-positive IECs in the small intestine of *CFLARs* Tg embryonic mice, but not in wild-type mice (Fig. 1B). Of note, deletion of *Rorc* depleted RORγt$^+$ cells, resulting in abrogation of *Reg3b* expression in the small intestine of *CFLARs* Tg mice [11]. These data together suggest that RORγt$^+$ cells induce production of Reg3β by IECs along with phosphorylation of STAT3.

In contrast to the absence of Reg3β expression at the normal embryonic stages, Reg3β was abundantly expressed in the small intestine, but not the colon of adult wild-type mice (Fig. 1C). Moreover, Reg3β expression correlated with phosphorylation of STAT3 (Fig. 1C). Consistent with these data, the expression of *Reg3b* and *Reg3g* was highly elevated in the small intestine but not in the colon of adult wild-type mice (Fig. 1D).

3.2. Generation of *Reg3b*$^{-/-}$ and *Reg3g*$^{-/-}$ mice by the CRISPR-Cas9 method

Although we previously reported that deletion of *Rorc* or *Il22* attenuates embryonic lethality in *CFLARs* Tg mice [11], whether elevated Reg3β *per se* attenuates or exacerbates ileitis in *CFLARs* Tg mice remains unclear. Moreover, we have found that *Reg3g* expression is highly elevated in the embryonic small intestine of *CFLARs* Tg mice [11] and in adult wild-type animals (Fig. 1D). Given that Reg3γ exhibits 70% amino acid sequence identity with Reg3β [22,23], one might surmise that Reg3β and Reg3γ could mutually compensate for function under certain conditions. Thus, we tried to generate *Reg3b* and *Reg3g* double-deficient mice by the *CRISPR-Cas9* method. We designed a single all-in-one *FokI-dCas9* vector that encoded four different guide RNAs targeting exon 3 of the *Reg3b* and *Reg3g* genes [20]. Although we did not generate *Reg3b* and *Reg3g* double-deficient mice, we independently generated two lines of *Reg3b*$^{-/-}$ mice and two lines of *Reg3g*$^{-/-}$ mice. Two lines of *Reg3b*$^{-/-}$ mice, designated as B12 and B52, harbored 29-bp and 32-bp deletions of exon 3 of *Reg3b*, respectively (Fig. 2A). By Western blotting and immunohistochemistry, we confirmed that Reg3β expression was abolished in the small intestine of *Reg3b*$^{-/-}$ mice (Fig. 2B and C). *Reg3b*$^{-/-}$ mice grew without apparent abnormalities of the small intestine or colon (Fig. 2D).

Two lines of *Reg3g*$^{-/-}$ mice, designated as G151 and G152, harbored 4-bp and 25-bp deletions of exon 3 of *Reg3g*, respectively (Fig. 3A). Reg3γ expression was abolished in the small intestine of *Reg3g*$^{-/-}$ mice (Fig. 3B). Notably, both lines also contained an in-frame deletion of exon 3 of *Reg3b*, resulting in generation of truncated forms of Reg3β (Reg3βΔ; Fig. 3C). Similar to *Reg3b*$^{-/-}$ mice, *Reg3bΔ;Reg3g*$^{-/-}$ mice grew without apparent abnormalities of the small intestine or colon (Fig. 3D). Because it was not clear whether Reg3βΔ would retain or lose Reg3β function, we focused on *Reg3b*$^{-/-}$ mice for subsequent experiments.

3.3. Deletion of Reg3b exacerbates the embryonic lethality of $X^{CF}X$ mice

We next crossed *Reg3b*$^{-/-}$ mice with *CFLARs* Tg mice. Numbers of $X^{CF}X$ mice on a *Reg3b*$^{-/-}$ background were reduced compared to those on a *Reg3b*$^{+/+}$ background (B12: 13.6% vs. 40.9%; B52: 11.4% vs. 48.6%; Table 1). Because relatively young *X^{CF}X;Reg3b*$^{+/-}$ mice became

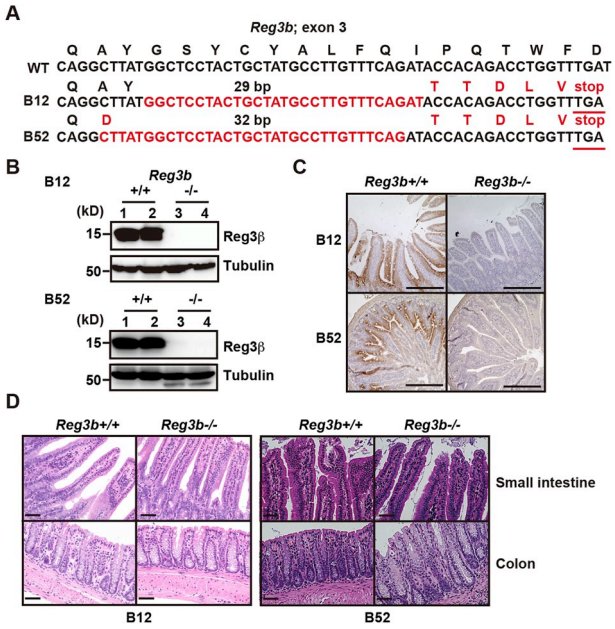

Fig. 2. Generation of *Reg3b*$^{-/-}$ mice. (A) Deletion of exon 3 of *Reg3b* genes in two lines of *Reg3b*$^{-/-}$ mice. Red characters indicate deleted nucleotides and mutated amino acids. (B) Tissue extracts were prepared from the small intestine of 8- to 12-week-old *Reg3b*$^{+/+}$ and *Reg3b*$^{-/-}$ mice and examined by Western blotting with the indicated antibodies. Each number indicates an individual mouse. Results represent two independent experiments. (C, D) Paraffin-embedded tissue sections of the small intestine and colon of 8- to 12-week-old *Reg3b*$^{+/+}$ and *Reg3b*$^{-/-}$ mice were stained with anti-Reg3β antibody (for the small intestine) (C) or Hematoxylin & Eosin (H&E) (for the small intestine and colon) (D). Scale bars, 100 μm.

infertile (data not shown), we could not obtain sufficient *X^{CF}X;Reg3b*$^{-/-}$ mice for timed mating with *XY;Reg3b*$^{+/-}$ animals. Thus, there were technical difficulties with comparing ileitis severity in *X^{CF}X;Reg3b*$^{+/-}$ and *X^{CF}X;Reg3b*$^{-/-}$ mice in the same litter. Nevertheless, these results suggest that the absence of Reg3β exacerbated embryonic lethality in $X^{CF}X$ mice.

3.4. DSS-induced colitis is exacerbated in *Reg3b*$^{-/-}$ mice

Previous studies have shown that Reg3β is involved in tissue homeostasis of the heart, liver, and intestine [5,24,25]. However, whether Reg3β plays a protective role in DSS-induced colitis was unclear. To address this issue, *Reg3b*$^{-/-}$ mice were administered with 1.5% DSS in drinking water for 5 days, which then was changed to regular water. Although Reg3β expression was undetectable in colon samples of untreated wild-type mice, the expression of *Reg3b* and *Reg3g* was elevated in colon samples from DSS-treated wild-type animals (Fig. 4A).

Body weight loss is a hallmark of the severity of colitis in DSS-treated mice, so we measured and compared body weights of two lines of *Reg3b*$^{-/-}$ mice to those of control wild-type mice cohoused with *Reg3b*$^{-/-}$ mice for at least 2 weeks. As shown in Fig. 4B and C, body weight loss was exacerbated in line B52 and to a lesser extent in line B12 of *Reg3b*$^{-/-}$ mice compared to wild-type mice. Histological analysis revealed that IECs were still detached from the villi of colon samples from *Reg3b*$^{-/-}$ mice, whereas wild-type mice almost completely recovered from epithelial injury of the colon (Fig. 4D). Moreover, submucosal edema was still observed in colon samples of *Reg3b*$^{-/-}$ mice (Fig. 4D).

To investigate the mechanism underlying exacerbation of colitis in *Reg3b*$^{-/-}$ mice, we analyzed infiltrated cells in the colons of wild-type and *Reg3b*$^{-/-}$ animals on day 8 after DSS administration. Lines B12

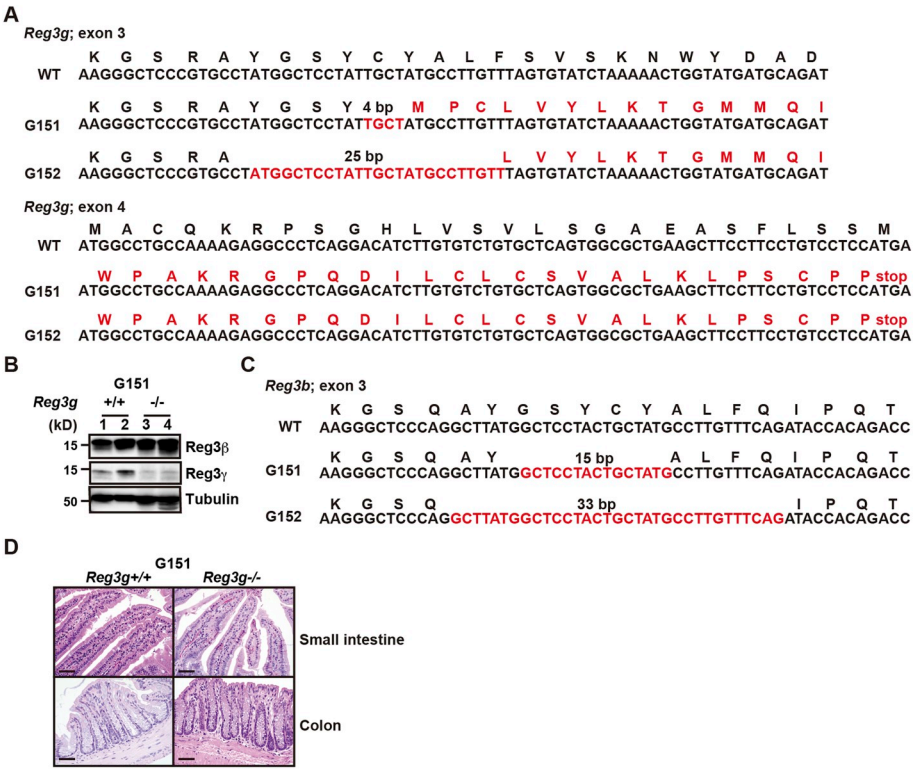

Fig. 3. Generation of *Reg3g*$^{-/-}$ mice. (A) Deletion of exon 3 of *Reg3g* genes in two lines of *Reg3g*$^{-/-}$ mice. Red characters indicate deleted nucleotides and mutated amino acids. (B) Tissue extracts were prepared from the small intestine of 8- to 12-week-old *Reg3g*$^{+/+}$ and *Reg3g*$^{-/-}$ mice (line G151) and examined by Western blotting with the indicated antibodies. Each number indicates an individual mouse. Results represent two independent experiments. (C) In-frame deletion of exon 3 of *Reg3b* in two lines of *Reg3g*$^{-/-}$ mice. Red characters indicate the deleted nucleotides. (D) Paraffin-embedded tissue sections of the small intestine and colon of 8- to 12-week-old *Reg3g*$^{+/+}$ and *Reg3g*$^{-/-}$ mice (line G151) were stained with H&E. Scale bars, 100 μm.

Table 1
Deletion of *Reg3b* exacerbates lethality of *CFLARs* Tg mice.

Line B12		*Reg3b*			Total
Genotypes		+/+	+/−	−/−	
XY	No.	17	20	10	47
	%	36.2	42.6	21.3	100
$X^{CF}Y$	No.	0	1	0	1
	%	0	100	0	100
XX	No.	20	24	7	51
	%	39.2	47.1	13.7	100
$X^{CF}X$	No.	9	10	3	22
	%	40.9	45.5	13.6	100
Line B52 Genotypes		*Reg3b* +/+	+/−	−/−	Total
XY	No.	23	39	14	76
	%	30.3	51.3	18.4	100
$X^{CF}Y$	No.	0	0	0	0
	%	0	0	0	0
XX	No.	30	44	17	91
	%	33.0	48.4	18.7	100
$X^{CF}X$	No.	17	14	4	35
	%	48.6	40.0	11.4	100

Female *CFLARs* Tg mice were crossed with two lines (B12 and B52) of *Reg3b*$^{-/-}$ mice and genotypes of the progeny were determined by PCR at 3–4 weeks after birth.

and B52 of *Reg3b*$^{-/-}$ mice had shown a similar phenotype after DSS treatment, so we focused on line B52 of *Reg3b*$^{-/-}$ mice for subsequent analysis. As shown in Fig. 4E and F, numbers of infiltrated neutrophils (CD11b^{+}Ly-6G^{+} cells) were significantly increased in the colons of *Reg3b*$^{-/-}$ compared to wild-type mice.

Given that DSS-induced colitis was exacerbated in *Reg3b*$^{-/-}$ mice, one might surmise that inflammation might be enhanced or tissue repair processes might be delayed in the colon of *Reg3b*$^{-/-}$ mice. We first investigated the expression of inflammatory cytokines. The expression of *Il6*, but not *Tnf*, *Il11*,*Il17a, Il22, or Reg3g* was elevated in the colon of *Reg3b*$^{-/-}$ mice compared to wild-type mice (Fig. 4G). Since M2-type macrophages are involved in tissue repair process [6,26], we then examined the expression of M2-type macrophage markers such as *Arginase-1 (Arg1)*, *Chitinase-like 3 (Chil3), Mannose receptor C-type 1 (Mrc1),* and *Resistin-like alpha (Retnla)*. The expression of *Chil3*, but not *Arg1, Mrc1,* or *Retnla* was highly elevated in the colon of *Reg3b*$^{-/-}$ mice compared to wild-type mice (Fig. 4G), suggesting that elevated expression of *Chil3* might be correlated with exacerbation of colitis in *Reg3b*$^{-/-}$ mice.

4. Discussion

In the present study, we generated *Reg3b*$^{-/-}$ mice and showed that deletion of *Reg3b* exacerbated ileitis in *CFLARs* Tg mice. Moreover, DSS-induced colitis was exacerbated in *Reg3b*$^{-/-}$ compared to wild-type mice, suggesting attenuation of colitis and ileitis is a result of Reg3β's real function.

We recently reported that expression of *Reg3b* and *Reg3g* is elevated in the *CFLARs* Tg embryonic small intestine but not in wild-type mice [11]. Given that Reg3β is involved in tissue repair processes, based on various tissue injury models [4,5,24,25], we surmised that deletion of *Reg3b* might exacerbate ileitis in *CFLARs* Tg mice. As expected, deletion of *Reg3b* enhanced embryonic lethality in these animals. Given that *CFLARs* Tg mice develop ileitis in utero, commensal bacteria do not appear to contribute to the development of ileitis in *CFLARs* Tg mice [11]. Thus, Reg3β might attenuate ileitis in a manner independent of antimicrobial function. Consistent with this notion, dedifferentiated cardiomyocytes release Reg3β that recruits macrophages, promoting myocardial healing after ischemic injury [5].

Ileitis in *CFLARs* Tg embryos is reminiscent of the necrotizing enterocolitis that affects extremely preterm infants [27,28]. Necrotizing enterocolitis is characterized by dilatation of the intestine, destruction of the villus structures, and intestinal bleeding. Notably, the expression of *Reg3b* was absent in wild-type embryonic small intestine, but its expression was extremely high in the small intestines of adult wild-type mice. Assuming that Reg3β has a protective role in the development of

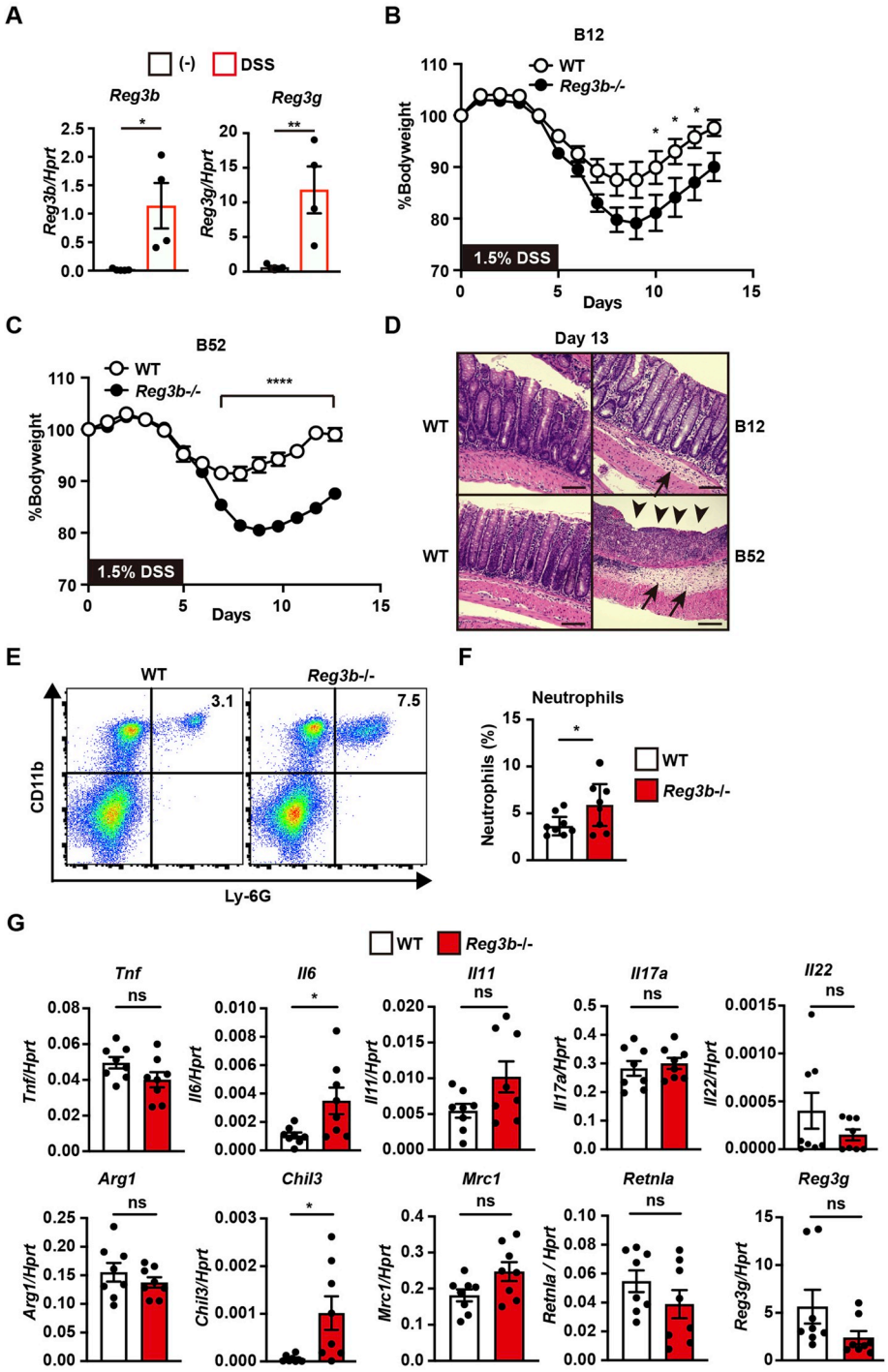

Fig. 4. Exacerbation of DSS-induced colitis in *Reg3b*$^{-/-}$ mice. Two lines of 8- to 12-week-old of *Reg3b*$^{-/-}$ mice and respective control wild-type mice were administered with 1.5% DSS in drinking water for 5 days, which then was changed to regular water. (A) RNA was prepared from colon samples of wild-type mice on day 8 after DSS treatment, and the expression of *Reg3b* and *Reg3g* was determined by qPCR. Results are mean ± SEM (n = 4 mice). Statistical significance was determined using the two-tailed unpaired Student's *t*-test. **P* < 0.05, ***P* < 0.01. (B, C) The average body weight is shown as the percentage relative to the initial value. Results are mean ± SEM (n = 9–10 mice). Pooled results of two independent experiments are shown. Statistical significance was determined using repeated measures ANOVA. **P* < 0.05, *****P* < 0.0001. (D) Colonic sections of the indicated mice on day 13 after DSS treatment were stained with H&E (n = 4 mice per genotype). Black arrows and arrowheads indicate submucosal edema and the inflamed colonic mucosa lacking epithelial cells, respectively. Scale bars, 100 μm. (E, F) Numbers of infiltrated neutrophils increased in the colon of *Reg3b*$^{-/-}$ mice on day 8 after DSS treatment. Single cell suspension was prepared from the colon of wild-type and *Reg3b*$^{-/-}$ mice. Cells were stained with the indicated antibodies, and percentages of CD11b^{+}Ly-6G^{+} cells (neutrophils) among CD45.2-positive cells were calculated. The results are shown in the right upper corner. Representative profiles of flow cytometry (E). Results are mean ± SEM (n = 7 mice) (F). Pooled results of two independent experiments are shown. Statistical significance was determined using the two-tailed unpaired Student's *t*-test. **P* < 0.05. (G) Expression of the indicated genes in the colon of wild-type and *Reg3b*$^{-/-}$ mice on day 8 after DSS treatment was determined by qPCR. Results are mean of ± SEM (n = 8 mice). Pooled results of two independent experiments are shown. Statistical significance was determined using the two-tailed unpaired Student's *t*-test. **P* < 0.05, ns, not significant.

ileitis, low expression levels of *Reg3b* might be causative in the development of necrotizing ileitis in extremely preterm infants in whom *Reg3b* expression is thought to be quite low.

Our preliminary experiments revealed that crossing *CFLARs* Tg mice with *Reg3bΔ;Reg3g*$^{-/-}$ mice did not exacerbate the *CFLARs* Tg embryonic lethality (data not shown). We cannot formally exclude the possibility that deleting 5 or 11 amino acids of Reg3β protein might modulate Reg3β function. However, these results suggest that Reg3β and Reg3γ have different functions in terms of attenuation of ileitis in *CFLARs* Tg mice. Generation of single *Reg3g*$^{-/-}$ mice will be required to further substantiate our preliminary results. Moreover, generation of compound knockout mice of *Reg3b* and *Reg3g* might also be required to elucidate the functions of Reg3β and Reg3γ under various pathological conditions in vivo.

In contrast to Reg3β, deletion of *Rorc* or *Il22* substantially rescued the embryonic lethality of $X^{CF}Y$ mice [11]. These results appeared to be inconsistent because *Rorc* and *Il22* genes are essential for induction of *Reg3b* and *Reg3g* by the ILC3s/IL-22–dependent pathway [11]. One plausible explanation is that deletion of *Rorc* and *Il22* suppresses apoptosis-promoting genes such as *Duox2* [29] that are regulated by this pathway, attenuating the embryonic lethal phenotype of $X^{CF}Y$ mice.

Our present study showed that DSS-induced colitis was exacerbated in *Reg3b*$^{-/-}$ mice. We found that submucosal edema was still present in colons of *Reg3b*$^{-/-}$ mice on day 13 after DSS treatment, but this edema had completely disappeared in wild-type animals. Given that intestinal

infection by *Salmonella* is exacerbated in *Reg3b*$^{-/-}$ mice [25], it is reasonable to surmise that Reg3β might act as an antimicrobial protein in limiting the penetration of commensal bacteria in the colon after DSS treatment. Consistent with this possibility, the numbers of infiltrated neutrophils and the expression of *Il6* were significantly increased in the colons of *Reg3b*$^{-/-}$ mice compared to wild-type animals. Previous studies reported that Reg3β is involved in tissue repair processes through recruiting macrophages [5], and that depletion of Ym1^{+} M2-type macrophages delays the recovery from DSS-induced colitis in mice [26]. We found that the expression of *Chil3*, but not other M2-type macrophage markers including, *Arg1*, *Mrc1*, or *Retnla,* was elevated in the colon of *Reg3b*$^{-/-}$ mice. Given that neutrophils and inflammatory macrophage highly express *Chil3* under certain conditions [30,31], these results suggest that elevated expression of *Chil3* might only represent enhanced inflammation characterized by increased infiltration of neutrophils or inflammatory macrophages in the colon of *Reg3b*$^{-/-}$ mice. However, we cannot formally exclude the possibility that recruitment of M2-type macrophages specifically expressed *Chil3*, but not other M2-type macrophage markers, might be delayed and still stay in the colon of *Reg3b*$^{-/-}$ mice compared to wild-type mice due to the absence of Reg3β. To discriminate these two possibilities, we need to compare the kinetics of the expression of various M2-type macrophage markers including *Chil3*, and recruitment of Ym1^{+} macrophages in the colon of wild-type and *Reg3b*$^{-/-}$ mice after DSS treatment.

CRediT authorship contribution statement

Ryodai Shindo: Investigation. **Takaharu Katagiri:** Investigation. **Sachiko Komazawa-Sakon:** Investigation. **Masaki Ohmuraya:** Resources. **Wakami Takeda:** Investigation. **Yoshiko Nakagawa:** Resources. **Naomi Nakagata:** Resources. **Tetsushi Sakuma:** Resources. **Takashi Yamamoto:** Resources. **Chiharu Nishiyama:** Supervision. **Takashi Nishina:** Investigation. **Soh Yamazaki:** Writing - review & editing. **Hideto Kameda:** Supervision. **Hiroyasu Nakano:** Writing - original draft, Writing - review & editing.

Declaration of competing interest

The authors declare that no competing interests exist.

Acknowledgments

We thank H. Kiyama for anti-Reg3γ antibody. This work was supported in part by Grants-in-Aid for Scientific Research (B) 17H04069 (to HN) and Challenging Exploratory Research 17K19533 (to HN) from the Japan Society for the Promotion of Science, and Scientific Research on Innovative areas 26110003 (to HN), the Japan Agency for Medical Research and Development (AMED) through AMED-CREST (grant number JP19gm1210002, to HN), and Private University Research Branding project (to HN) from MEXT (Ministry of Education, Culture, Sports, Science and Technology), Japan.

Appendix A. Supplementary data

Supplementary data to this article can be found online at https://doi.org/10.1016/j.bbrep.2020.100738.

References

[1] D. Viterbo, M.H. Bluth, C.M. Mueller, M.E. Zenilman, Mutational characterization of pancreatitis-associated protein 2 domains involved in mediating cytokine secretion in macrophages and the NF-kappaB pathway, J. Immunol. 181 (2008) 1959–1968, https://doi.org/10.4049/jimmunol.181.3.1959.

[2] A. Parikh, A.F. Stephan, E.S. Tzanakakis, Regenerating proteins and their expression, regulation and signaling, Biomol. Concepts 3 (2012) 57–70, https://doi.org/10.1515/bmc.2011.055.

[3] S. Matsumoto, H. Konishi, R. Maeda, S. Kiryu-Seo, H. Kiyama, Expression analysis of the regenerating gene (Reg) family members Reg-IIIbeta and Reg-IIIgamma in the mouse during development, J. Comp. Neurol. 520 (2012) 479–494, https://doi.org/10.1002/cne.22705.

[4] M. Gironella, C. Calvo, A. Fernandez, D. Closa, J.L. Iovanna, J. Rosello-Catafau, E. Folch-Puy, Reg3beta deficiency impairs pancreatic tumor growth by skewing macrophage polarization, Canc. Res. 73 (2013) 5682–5694, https://doi.org/10.1158/0008-5472.CAN-12-3057.

[5] H. Lorchner, J. Poling, P. Gajawada, Y. Hou, V. Polyakova, S. Kostin, J.M. Adrian-Segarra, T. Boettger, A. Wietelmann, H. Warnecke, M. Richter, T. Kubin, T. Braun, Myocardial healing requires Reg3beta-dependent accumulation of macrophages in the ischemic heart, Nat. Med. 21 (2015) 353–362, https://doi.org/10.1038/nm.3816.

[6] P.J. Murray, J.E. Allen, S.K. Biswas, E.A. Fisher, D.W. Gilroy, S. Goerdt, S. Gordon, J.A. Hamilton, L.B. Ivashkiv, T. Lawrence, M. Locati, A. Mantovani, F.O. Martinez, J.L. Mege, D.M. Mosser, G. Natoli, J.P. Saeij, J.L. Schultze, K.A. Shirey, A. Sica, J. Suttles, I. Udalova, J.A. van Ginderachter, S.N. Vogel, T.A. Wynn, Macrophage activation and polarization: nomenclature and experimental guidelines, Immunity 41 (2014) 14–20, https://doi.org/10.1016/j.immuni.2014.06.008.

[7] L.M. Loonen, E.H. Stolte, M.T. Jaklofsky, M. Meijerink, J. Dekker, P. van Baarlen, J.M. Wells, REG3gamma-deficient mice have altered mucus distribution and increased mucosal inflammatory responses to the microbiota and enteric pathogens in the ileum, Mucosal Immunol. 7 (2014) 939–947, https://doi.org/10.1038/mi.2013.109.

[8] S. Takasawa, C. Tsuchida, S. Sakuramoto-Tsuchida, M. Takeda, A. Itaya-Hironaka, A. Yamauchi, M. Misu, R. Shobatake, T. Uchiyama, M. Makino, C. Ohbayashi, Expression of human REG family genes in inflammatory bowel disease and their molecular mechanism, Immunol. Res. 66 (2018) 800–805, https://doi.org/10.1007/s12026-019-9067-2.

[9] E. Montaldo, K. Juelke, C. Romagnani, Group 3 innate lymphoid cells (ILC3s): origin, differentiation, and plasticity in humans and mice, Eur. J. Immunol. 45 (2015) 2171–2182, https://doi.org/10.1002/eji.201545598.

[10] W. Huang, D.R. Littman, Regulation of RORgammat in inflammatory lymphoid cell differentiation, Cold Spring Harbor Symp. Quant. Biol. 80 (2015) 257–263, https://doi.org/10.1101/sqb.2015.80.027615.

[11] R. Shindo, M. Ohmuraya, S. Komazawa-Sakon, S. Miyake, Y. Deguchi, S. Yamazaki, T. Nishina, T. Yoshimoto, S. Kakuta, M. Koike, Y. Uchiyama, H. Konishi, H. Kiyama, T. Mikami, K. Moriwaki, K. Araki, H. Nakano, Necroptosis of intestinal epithelial cells induces type 3 innate lymphoid cell-dependent lethal ileitis, iScience 15 (2019) 536–551, https://doi.org/10.1016/j.isci.2019.05.011.

[12] J. Yuan, Divergence from a dedicated cellular suicide mechanism: exploring the evolution of cell death, Mol. Cell. 23 (2006) 1–12, https://doi.org/10.1016/j.molcel.2006.06.008.

[13] M. Pasparakis, P. Vandenabeele, Necroptosis and its role in inflammation, Nature 517 (2015) 311–320, https://doi.org/10.1038/nature14191.

[14] R. Weinlich, A. Oberst, H.M. Beere, D.R. Green, Necroptosis in development, inflammation and disease, Nat. Rev. Mol. Cell Biol. 18 (2017) 127–136, https://doi.org/10.1038/nrm.2016.149.

[15] R.C. Budd, W.C. Yeh, J. Tschopp, cFLIP regulation of lymphocyte activation and development, Nat. Rev. Immunol. 6 (2006) 196–204.

[16] H. Nakano, X. Piao, R. Shindo, S. Komazawa-Sakon, Cellular FLICE-inhibitory protein regulates tissue homeostasis, Curr. Top. Microbiol. Immunol. 403 (2017) 119–141, https://doi.org/10.1007/82_2015_448.

[17] D. Panayotova-Dimitrova, M. Feoktistova, M. Ploesser, B. Kellert, M. Hupe, S. Horn, R. Makarov, F. Jensen, S. Porubsky, A. Schmieder, A.C. Zenclussen, A. Marx, A. Kerstan, P. Geserick, Y.W. He, M. Leverkus, cFLIP regulates skin homeostasis and protects against TNF-induced keratinocyte apoptosis, Cell Rep. 5 (2013) 397–408, https://doi.org/10.1016/j.celrep.2013.09.035.

[18] A. Oberst, C.P. Dillon, R. Weinlich, L.L. McCormick, P. Fitzgerald, C. Pop, R. Hakem, G.S. Salvesen, D.R. Green, Catalytic activity of the caspase-8-FLIP(L) complex inhibits RIPK3-dependent necrosis, Nature 471 (2011) 363–367 nature09852 [pii] 10.1038/nature09852.

[19] G. Eberl, S. Marmon, M.J. Sunshine, P.D. Rennert, Y. Choi, D.R. Littman, An essential function for the nuclear receptor RORgamma(t) in the generation of fetal lymphoid tissue inducer cells, Nat. Immunol. 5 (2004) 64–73, https://doi.org/10.1038/ni1022.

[20] Y. Nakagawa, T. Sakuma, T. Sakamoto, M. Ohmuraya, N. Nakagata, T. Yamamoto, Production of knockout mice by DNA microinjection of various CRISPR/Cas9 vectors into freeze-thawed fertilized oocytes, BMC Biotechnol. 15 (2015) 33, https://doi.org/10.1186/s12896-015-0144-x.

[21] S. Yamazaki, Y. Tanaka, H. Araki, A. Kohda, F. Sanematsu, T. Arasaki, X. Duan, F. Miura, T. Katagiri, R. Shindo, H. Nakano, T. Ito, Y. Fukui, S. Endo, H. Sumimoto, The AP-1 transcription factor JunB is required for Th17 cell differentiation, Sci. Rep. 7 (2017) 17402, https://doi.org/10.1038/s41598-017-17597-3.

[22] M. Abe, K. Nata, T. Akiyama, N.J. Shervani, S. Kobayashi, T. Tomioka-Kumagai, S. Ito, S. Takasawa, H. Okamoto, Identification of a novel Reg family gene, Reg IIIdelta, and mapping of all three types of Reg family gene in a 75 kilobase mouse genomic region, Gene 246 (2000) 111–122.

[23] Y.W. Zhang, L.S. Ding, M.D. Lai, Reg gene family and human diseases, World J. Gastroenterol. 9 (2003) 2635–2641, https://doi.org/10.3748/wjg.v9.i12.2635.

[24] L. Wang, D.E. Fouts, P. Starkel, P. Hartmann, P. Chen, C. Llorente, J. DePew, K. Moncera, S.B. Ho, D.A. Brenner, L.V. Hooper, B. Schnabl, Intestinal REG3 lectins protect against alcoholic steatohepatitis by reducing mucosa-associated microbiota and preventing bacterial translocation, Cell Host Microbe 19 (2016) 227–239, https://doi.org/10.1016/j.chom.2016.01.003.

[25] M.T. van Ampting, L.M. Loonen, A.J. Schonewille, I. Konings, C. Vink, J. Iovanna, M. Chamaillard, J. Dekker, R. van der Meer, J.M. Wells, I.M. Bovee-Oudenhoven,

Intestinally secreted C-type lectin Reg3b attenuates salmonellosis but not listeriosis in mice, Infect. Immun. 80 (2012) 1115–1120, https://doi.org/10.1128/IAI.06165-11.

[26] N. Ikeda, K. Asano, K. Kikuchi, Y. Uchida, H. Ikegami, R. Takagi, S. Yotsumoto, T. Shibuya, C. Makino-Okamura, H. Fukuyama, T. Watanabe, M. Ohmuraya, K. Araki, G. Nishitai, M. Tanaka, Emergence of immunoregulatory Ym1(+)Ly6C(hi) monocytes during recovery phase of tissue injury, Sci Immunol 3 (2018), https://doi.org/10.1126/sciimmunol.aat0207.

[27] J.C. Lim, J.M. Golden, H.R. Ford, Pathogenesis of neonatal necrotizing enterocolitis, Pediatr. Surg. Int. 31 (2015) 509–518, https://doi.org/10.1007/s00383-015-3697-9.

[28] S.M. Tanner, T.F. Berryhill, J.L. Ellenburg, T. Jilling, D.S. Cleveland, R.G. Lorenz, C.A. Martin, Pathogenesis of necrotizing enterocolitis: modeling the innate immune response, Am. J. Pathol. 185 (2015) 4–16, https://doi.org/10.1016/j.ajpath.2014.08.028.

[29] H. Grasberger, J. Gao, H. Nagao-Kitamoto, S. Kitamoto, M. Zhang, N. Kamada, K.A. Eaton, M. El-Zaatari, A.B. Shreiner, J.L. Merchant, C. Owyang, J.Y. Kao, Increased expression of DUOX2 is an epithelial response to mucosal dysbiosis required for immune homeostasis in mouse intestine, Gastroenterology 149 (2015) 1849–1859, https://doi.org/10.1053/j.gastro.2015.07.062.

[30] P. Ramachandran, A. Pellicoro, M.A. Vernon, L. Boulter, R.L. Aucott, A. Ali, S.N. Hartland, V.K. Snowdon, A. Cappon, T.T. Gordon-Walker, M.J. Williams, D.R. Dunbar, J.R. Manning, N. van Rooijen, J.A. Fallowfield, S.J. Forbes, J.P. Iredale, Differential Ly-6C expression identifies the recruited macrophage phenotype, which orchestrates the regression of murine liver fibrosis, Proc. Natl. Acad. Sci. U. S. A. 109 (2012) E3186–E3195, https://doi.org/10.1073/pnas.1119964109.

[31] M. Harbord, M. Novelli, B. Canas, D. Power, C. Davis, J. Godovac-Zimmermann, J. Roes, A.W. Segal, Ym1 is a neutrophil granule protein that crystallizes in p47phox-deficient mice, J. Biol. Chem. 277 (2002) 5468–5475, https://doi.org/10.1074/jbc.M110635200.